Science Immunology
AAAS

Supplementary Materials for

A Stk4-Foxp3-p65 transcriptional complex promotes T_{reg} cell activation and homeostasis

Ye Cui *et al.*

Corresponding author: Talal A. Chatila, talal.chatila@childrens.harvard.edu

Sci. Immunol. **7**, eabl8357 (2022)
DOI: 10.1126/sciimmunol.abl8357

The PDF file includes:

Other Supplementary Material for this manuscript includes the following:

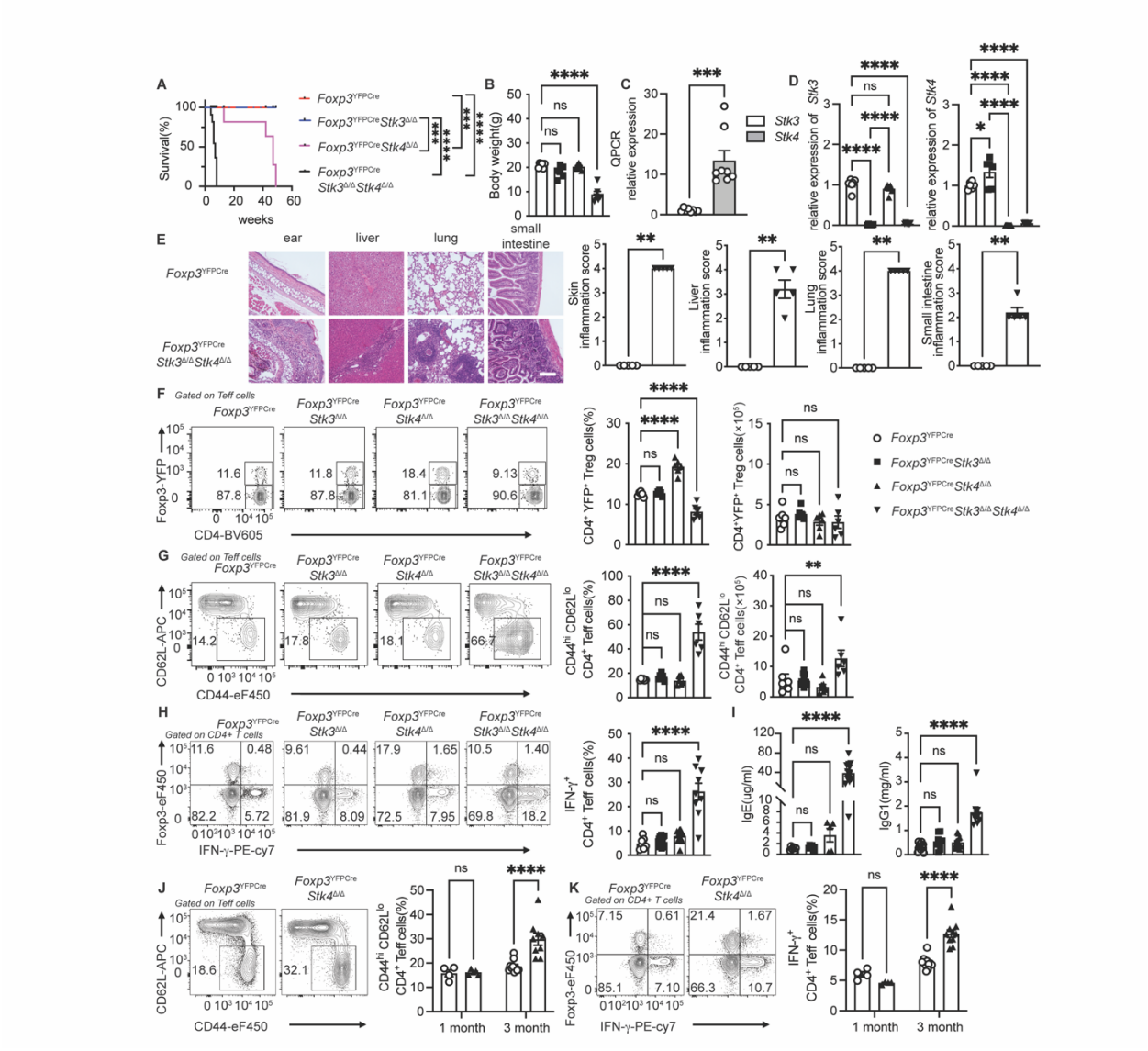

Fig. S1. *Stk3/4* deficiency in Treg cells causes fatal autoimmune lymphoproliferative disease. (**A**) Survival curve (*n*=11 per group) and (**B**) Body weight of *Foxp3*^{YFPCre}, *Foxp3*^{YFPCre}*Stk3*$^{Δ/Δ}$, *Foxp3*^{YFPCre}*Stk4*$^{Δ/Δ}$ and *Foxp3*^{YFPCre}*Stk3*$^{Δ/Δ}$*Stk4*$^{Δ/Δ}$ mice at 25–28 d of age (*n*=6 per group). The results represent a pool of five independent experiments. (**C**) Relative expression of *Stk3* and *Stk4* in Treg cells of *Foxp3*^{YFPCre} mice quantified by qPCR (*n*=8 per group). **(D)** Relative expression of *Stk3* and *Stk4* in Treg cells of *Foxp3*^{YFPCre}, *Foxp3*^{YFPCre}*Stk3*$^{Δ/Δ}$, *Foxp3*^{YFPCre}*Stk4*$^{Δ/Δ}$ and *Foxp3*^{YFPCre}*Stk3*$^{Δ/Δ}$*Stk4*$^{Δ/Δ}$

mice determined by qPCR (*n*=6 per group). (**E**) Representative histological pictures of hematoxylin and eosin staining (original magnification; ×200) and histological scores of the skin, lung, colon and liver from *Foxp3*^{YFPCre} (*n* = 5) *and Foxp3*^{YFPCre}*Stk3*$^{\Delta/\Delta}$*Stk4*$^{\Delta/\Delta}$ mice (*n* = 5). The results represent a pool of three independent experiments. (**F**) Representative flow cytometric analysis, cell frequencies and cell number of splenic CD4^{+}YFP^{+} Treg cells (*n*=6) from *Foxp3*^{YFPCre}, *Foxp3*^{YFPCre}*Stk3*$^{\Delta/\Delta}$, *Foxp3*^{YFPCre}*Stk4*$^{\Delta/\Delta}$ and *Foxp3*^{YFPCre}*Stk3*$^{\Delta/\Delta}$*Stk4*$^{\Delta/\Delta}$ mice. (**G**) Representative flow cytometric analysis, cell frequencies and cell number of splenic CD62L^{lo}CD44^{hi} CD4^{+} Teff cells (*n*=6-13) from *Foxp3*^{YFPCre}, *Foxp3*^{YFPCre}*Stk3*$^{\Delta/\Delta}$, *Foxp3*^{YFPCre}*Stk4*$^{\Delta/\Delta}$ and *Foxp3*^{YFPCre}*Stk3*$^{\Delta/\Delta}$*Stk4*$^{\Delta/\Delta}$ mice. (**H**) Representative flow cytometric analysis and cell frequencies of IFNγ^{+} Teff cells from *Foxp3*^{YFPCre} (*n*=7), *Foxp3*^{YFPCre}*Stk3*$^{\Delta/\Delta}$ (*n*=17), *Foxp3*^{YFPCre}*Stk4*$^{\Delta/\Delta}$ (*n*=15), *Foxp3*^{YFPCre}*Stk3*$^{\Delta/\Delta}$*Stk4*$^{\Delta/\Delta}$ (*n*=9) mice. The results represent pool of three independent experiments. (**I**) Total serum IgE (*n*=5-13) and IgG1 concentrations (*n*=8-12). in the respective groups. (**J** to **K**) Representative flow cytometric analysis of splenic CD62L^{lo}CD44^{hi} CD4^{+} Teff cells (J) and splenic IFNγ^{+} Teff cells (K) from 3-month-old *Foxp3*^{YFPCre} and *Foxp3*^{YFPCre}*Stk4*$^{\Delta/\Delta}$ mice. Cell frequencies of splenic CD62L^{lo}CD44^{hi} CD4^{+} Teff cells (**J**), splenic IFNγ^{+} Teff cells (**K**) from 1-month-old *Foxp3*^{YFPCre} (*n*=4 for CD62L^{lo}CD44^{hi} CD4^{+} Teff cells; *n*=4 for IFNγ^{+} Teff cells) and *Foxp3*^{YFPCre}*Stk4*$^{\Delta/\Delta}$ (*n*=5 for CD62L^{lo}CD44^{hi} CD4^{+} Teff cells; *n*=4 for IFNγ^{+} Teff cells) mice and 3-month-old *Foxp3*^{YFPCre} (*n*=10 for CD62L^{lo}CD44^{hi} CD4^{+} Teff cells; *n*=10 for IFNγ^{+} Teff cells) and *Foxp3*^{YFPCre}*Stk4*$^{\Delta/\Delta}$ (*n*=9 for CD62L^{lo}CD44^{hi} CD4^{+} Teff cells; *n*=10 for IFNγ^{+} Teff cells) mice. Each point represents one mouse. Error bars indicate the standard error of the means (S.E.M.). Statistical tests: ns: Not significant. ***P*<0.01, ***, *P*<0.005, ****,

P<0.0001. Log-rank test (**A**), one-way ANOVA with post-test analysis (**B**,**E** to **H**), Student's unpaired two tailed *t* test (**C**) or Mann Whitney test (**D**).

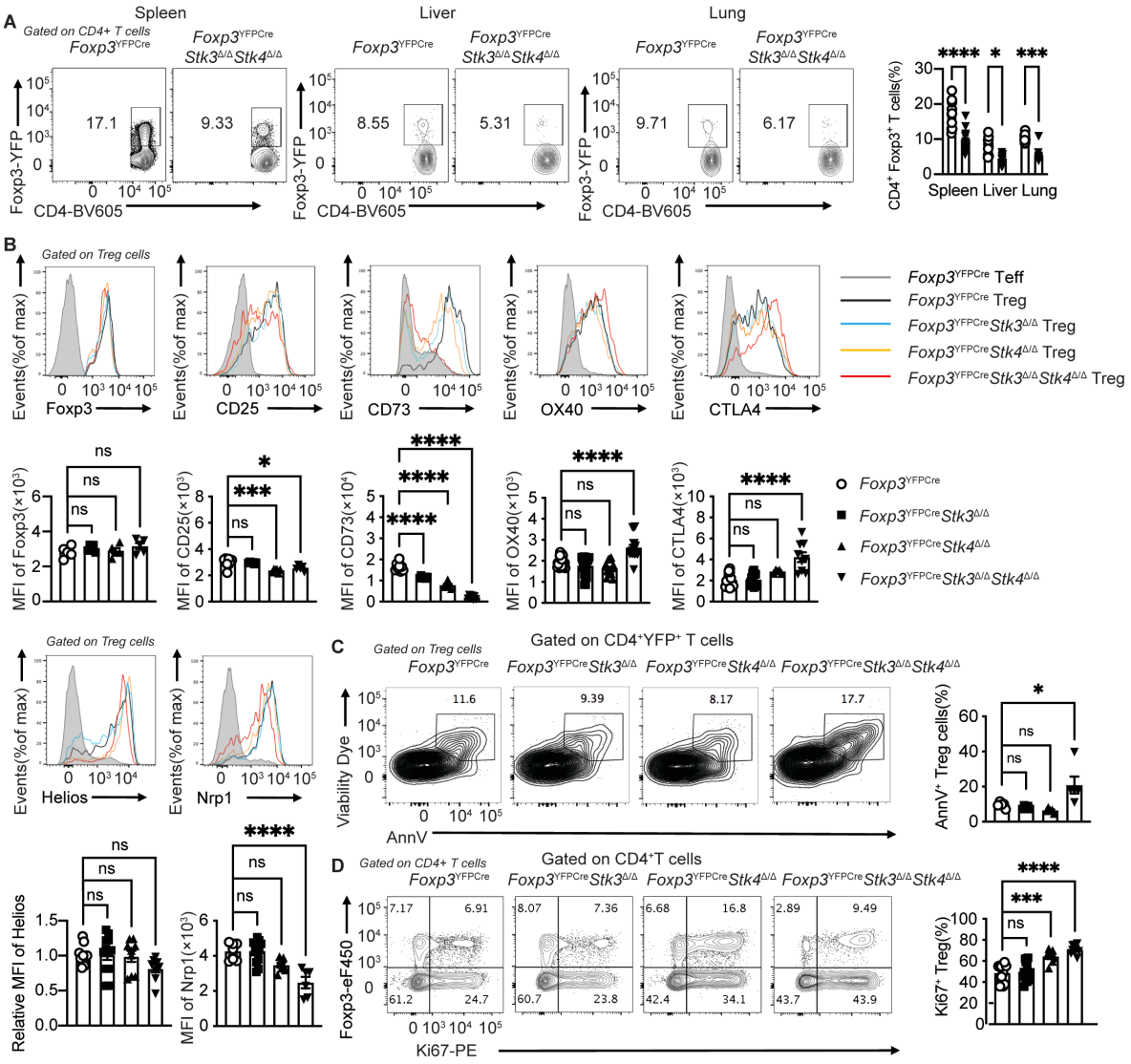

Fig. S2. Defective activation and survival of *Stk3/4*-deficient Treg cells. (**A**)Flow cytometric analysis and cell frequencies of CD4$^+$YFP$^+$ Treg cells from spleen, liver and lung of *Foxp3*^{YFPCre} (*n*=11) and *Foxp3*^{YFPCre}*Stk3*$^{Δ/Δ}$*Stk4*$^{Δ/Δ}$ mice (*n*=10). (**B**) Representative flow cytometric analysis and MFI of Foxp3 (*n*=5 per group), CD25 (*n*=5-8), CD73 (*n*=6-8), OX40 (*n*=14-25), CTLA-4 (*n*=5-15), Helios (*n*=9-12) and Nrp1 (*n*=6-13) of splenic Treg cells from *Foxp3*^{YFPCre}, *Foxp3*^{YFPCre}*Stk3*$^{Δ/Δ}$, *Foxp3*^{YFPCre}*Stk4*$^{Δ/Δ}$ and

Foxp3^{YFPCre}*Stk3*$^{\Delta/\Delta}$*Stk4*$^{\Delta/\Delta}$ mice. (**C** and **D**) Representative flow cytometric analysis and cell frequencies of splenic AnnexinV$^+$ Viability dye$^+$ Treg cells (**C**), splenic Ki67$^+$ Treg cells (**D**) from *Foxp3*^{YFPCre} (*n*=5 for AnnexinV$^+$ Viability dye$^+$ Treg cells; *n*=12 for Ki67$^+$ Treg cells), *Foxp3*^{YFPCre}*Stk3*$^{\Delta/\Delta}$ (*n*=5 for AnnexinV$^+$ Viability dye$^+$ Treg cells; *n*=15 for Ki67$^+$ Treg cells) , *Foxp3*^{YFPCre}*Stk4*$^{\Delta/\Delta}$ (*n*=5 for AnnexinV$^+$ Viability dye$^+$ Treg cells; *n*=7 for Ki67$^+$ Treg cells) and *Foxp3*^{YFPCre}*Stk3*$^{\Delta/\Delta}$*Stk4*$^{\Delta/\Delta}$ mice (*n*=5 for AnnexinV$^+$ Viability dye$^+$ Treg cells; *n*=10 for Ki67$^+$ Treg cells) mice. Each point represents one mouse. Error bars indicate the standard error of the means (S.E.M.). Statistical tests: ns: Not significant. ***P*<0.01, ***, *P*<0.005, ****, *P*<0.0001. two-way ANOVA with post-test analysis (**A**) or one-way ANOVA with post-test analysis (**B** to **D**). ns: Not significant, *, *P*<0.05, ****P*<0.005, ****, *P*<0.0001.

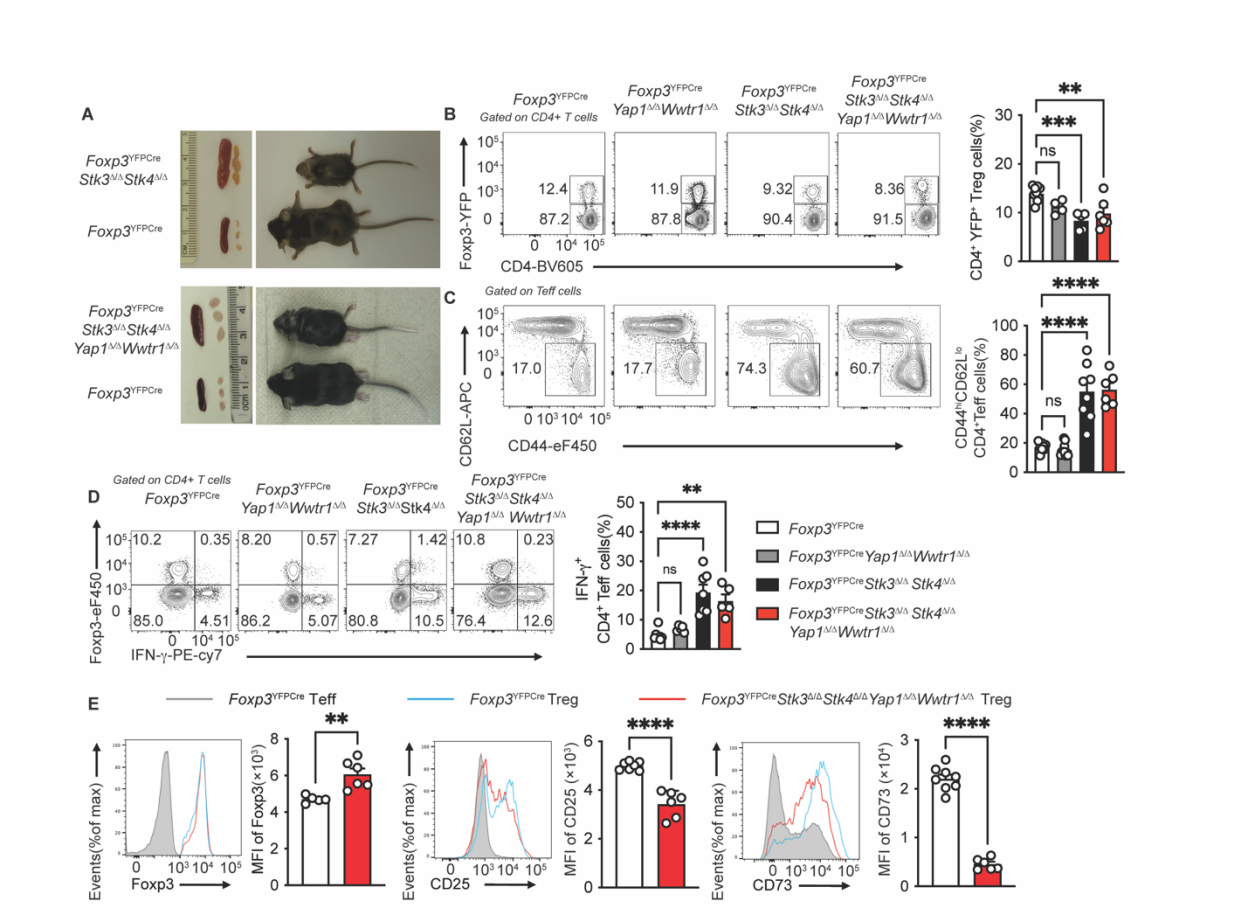

Fig. S3. Treg cell-specific inactivation of the Hippo pathway does not rescue the phenotype of *Foxp3*^{YFPCre}*Stk3*$^{\Delta/\Delta}$*Stk4*$^{\Delta/\Delta}$ mice. (**A**) Gross appearance of *Foxp3*^{YFPCre}*Stk3*$^{\Delta/\Delta}$*Stk4*$^{\Delta/\Delta}$, *Foxp3*^{YFPCre}*Stk3*$^{\Delta/\Delta}$*Stk4*$^{\Delta/\Delta}$*Yap1*$^{\Delta/\Delta}$*Wwtr1*$^{\Delta/\Delta}$ and control littermate mice, and their respective spleens and peripheral lymph nodes. (**B**) Representative flow cytometric analysis and cell frequencies of CD4^{+}YFP^{+} Treg cells from *Foxp3*^{YFPCre} (*n*=9); *Foxp3*^{YFPCre}*Yap1*$^{\Delta/\Delta}$*Wwtr1*$^{\Delta/\Delta}$ (*n*=5); *Foxp3*^{YFPCre}*Stk3*$^{\Delta/\Delta}$*Stk4*$^{\Delta/\Delta}$ (*n*=5); *Foxp3*^{YFPCre}*Stk3*$^{\Delta/\Delta}$*Stk4*$^{\Delta/\Delta}$*Yap1*$^{\Delta/\Delta}$*Wwtr1*$^{\Delta/\Delta}$ (*n*=6) mice. (**C**) Representative flow cytometric analysis and cell frequencies of CD62L^{lo}CD44^{hi} CD4^{+}YFP^{-} Teff cells of *Foxp3*^{YFPCre} (*n*=8), *Foxp3*^{YFPCre}*Yap1*$^{\Delta/\Delta}$*Wwtr1*$^{\Delta/\Delta}$ (*n*=10), *Foxp3*^{YFPCre}*Stk3*$^{\Delta/\Delta}$*Stk4*$^{\Delta/\Delta}$ (*n*=8) and *Foxp3*^{YFPCre}*Stk3*$^{\Delta/\Delta}$*Stk4*$^{\Delta/\Delta}$*Yap1*$^{\Delta/\Delta}$*Wwtr1*$^{\Delta/\Delta}$ (*n*=6) mice. (**D**) Flow cytometric analysis and

cell frequencies of splenic IFNγ^{+} Teff cells from *Foxp3*^{YFPCre} (*n*=7), *Foxp3*^{YFPCre}*Yap1*$^{Δ/Δ}$*Wwtr1*$^{Δ/Δ}$ (*n*=5), *Foxp3*^{YFPCre}*Stk3*$^{Δ/Δ}$*Stk4*$^{Δ/Δ}$ (*n*=7) and *Foxp3*^{YFPCre}*Stk3*$^{Δ/Δ}$*Stk4*$^{Δ/Δ}$ *Yap1*$^{Δ/Δ}$*Wwtr1*$^{Δ/Δ}$ mice (*n*=5). (**E**) Flow cytometric analysis and scatter plot representation of Foxp3 (*n*=5-6), CD25 (*n*=6-7) and CD73 (*n*=6-8) MFI in splenic Treg cells of *Foxp3*^{YFPCre} and *Foxp3*^{YFPCre}*Stk3*$^{Δ/Δ}$*Stk4*$^{Δ/Δ}$ *Yap1*$^{Δ/Δ}$*Wwtr1*$^{Δ/Δ}$ mice. Each point represents one mouse. Error bars indicate the standard error of the means (S.E.M.). Statistical tests: one-way ANOVA with post-test analysis (**B** to **D**) or Student's unpaired two tailed *t* test (**E**). ns: Not significant, **, *P*<0.01, ***P*<0.005, ****, *P*<0.0001.

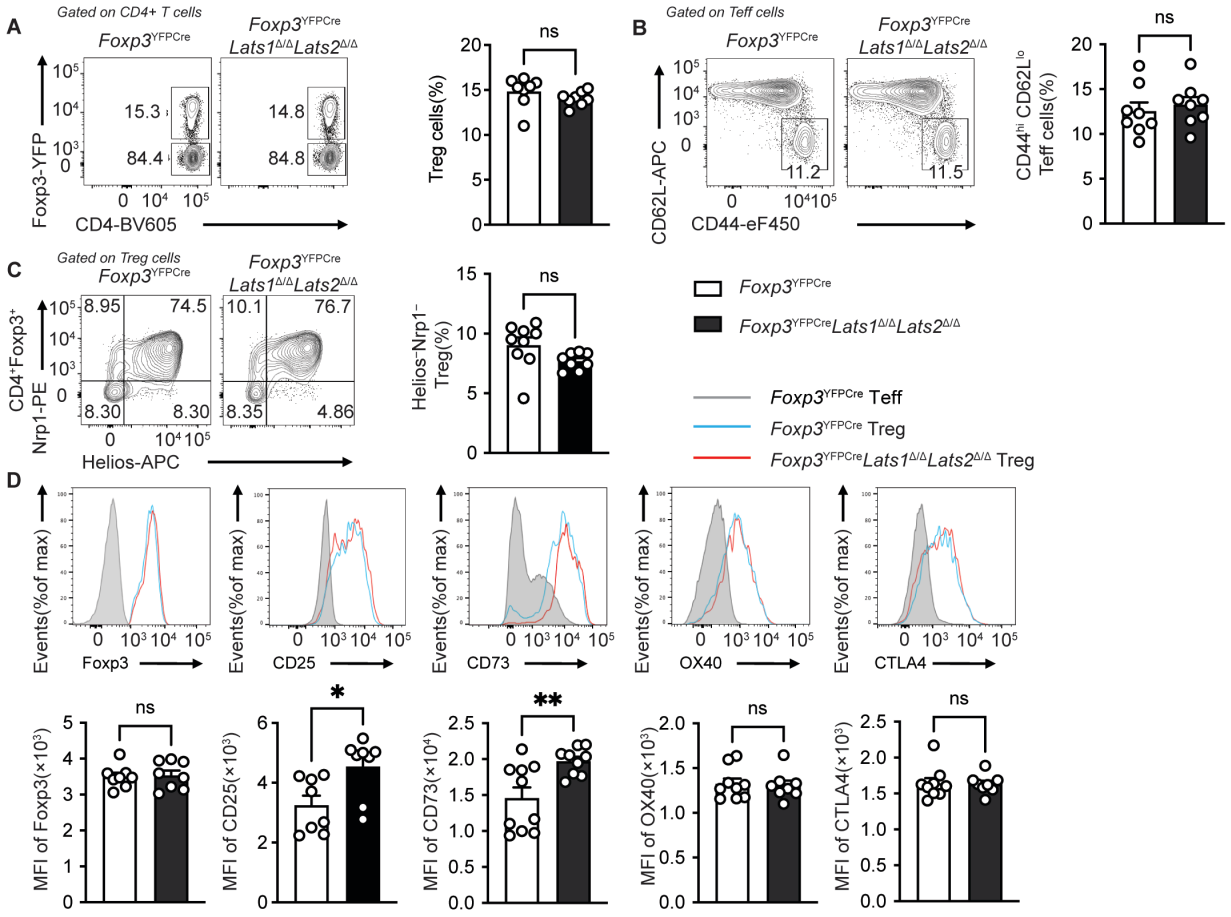

Fig. S4. Mice with Treg cell specific activation of the Hippo pathway do not

phenocopy *Foxp3*^{YFPCre}*Stk3*$^{\Delta/\Delta}$*Stk4*$^{\Delta/\Delta}$ mice. (**A**) Flow cytometric analysis and scatter plot representation of splenic Treg cells of *Foxp3*^{YFPCre} (*n*=8) and *Foxp3*^{YFPCre}*Lats1*$^{\Delta/\Delta}$*Lats2*$^{\Delta/\Delta}$ mice (*n*=8). (**B**) Flow cytometric analysis and scatter plot representation of CD44^{hi} CD62L^{lo} splenic Teff cells of *Foxp3*^{YFPCre} (*n*=8) and *Foxp3*^{YFPCre}*Lats1*$^{\Delta/\Delta}$*Lats2*$^{\Delta/\Delta}$ mice (*n*=8). (**C**) Flow cytometric analysis and scatter plot representation of splenic Helios^{-} Nrp1^{-} Treg cells of *Foxp3*^{YFPCre} (*n*=9) and *Foxp3*^{YFPCre}*Lats1*$^{\Delta/\Delta}$*Lats2*$^{\Delta/\Delta}$ mice (*n*=8). (**D**) Flow cytometric analysis and scatter plot representation of Foxp3 (*n*=8 per group), CD25 (*n*=8 per group), CD73 (*n*=9-10 per group), OX40 (*n*=8-9), CTLA-4 (*n*=8-9) MFI in splenic Treg cells of *Foxp3*^{YFPCre} and *Foxp3*^{YFPCre}*Lats1*$^{\Delta/\Delta}$*Lats2*$^{\Delta/\Delta}$ mice. Each point represents one mouse. Error bars indicate the standard error of the means (S.E.M.). Statistical tests: Student's unpaired two tailed *t* test (**A** to **D**). ns: Not significant, *, $P<0.05$, **$P<0.01$.

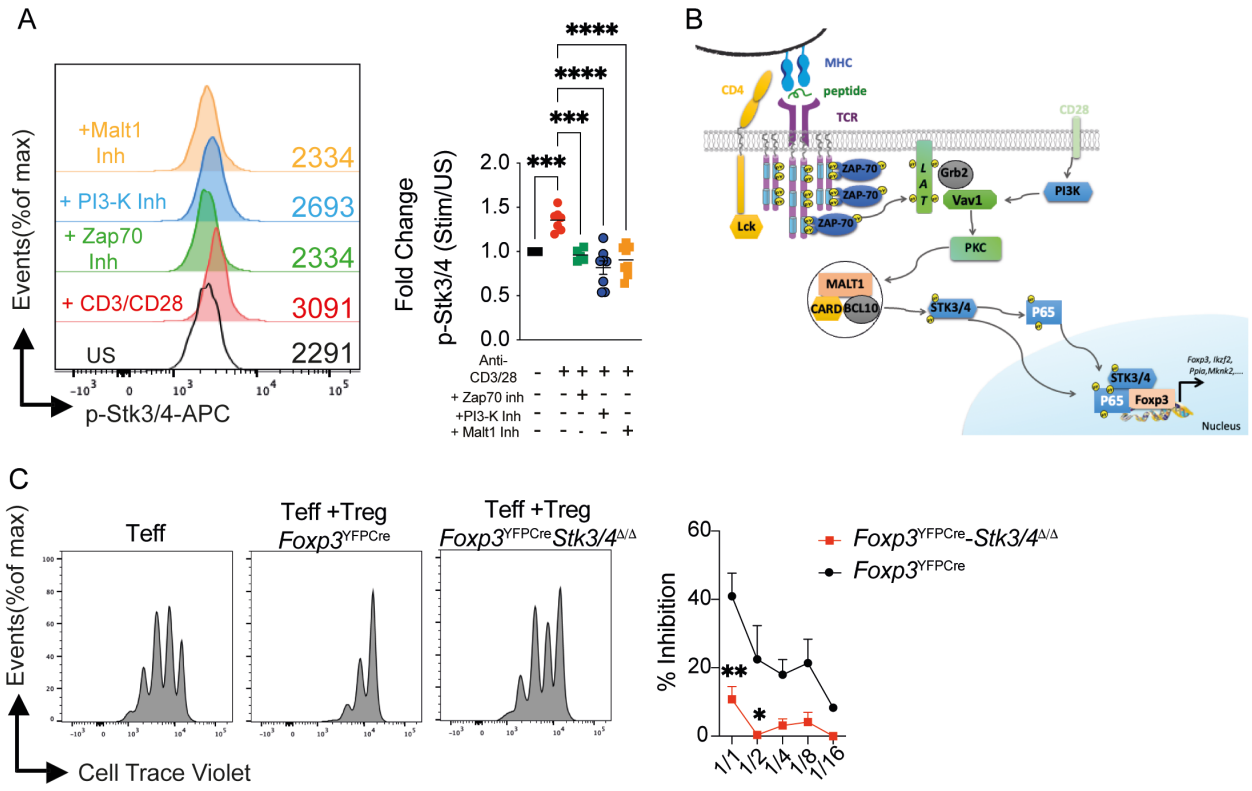

Fig. S5. TCR/CD28 signaling activates Stk4 by a Zap70, PI3K and Malt1-dependent mechanism to promote Treg suppressive function. (A) Representative histogram and Fold change (Stim/US) of phospho-MST1 expression on Treg cells in the respective treatment groups. **(B)** Proposed scheme of Stk4 activation following TCR stimulation. **(C)** *In vitro* suppression of WT CD4^{+} Teff cell proliferation of by *Foxp3*^{YFPCre} or *Foxp3*^{YFPCre}*Stk3/4*$^{\Delta/\Delta}$ Treg cells. Left: Representative histograms of the proliferation of Teff cells either alone or in the presence of Treg cells of the indicated genotypes at a 1:1 ratio; Right: Percent inhibition of Teff cell proliferation at different Treg cell/Teff cell ratios (n=3 replicates per point). ***p<0.001, ****p<0.0001 by one-way ANOVA and post-test analysis (A); **p<0.01 by repeat measure two-way ANOVA (C).

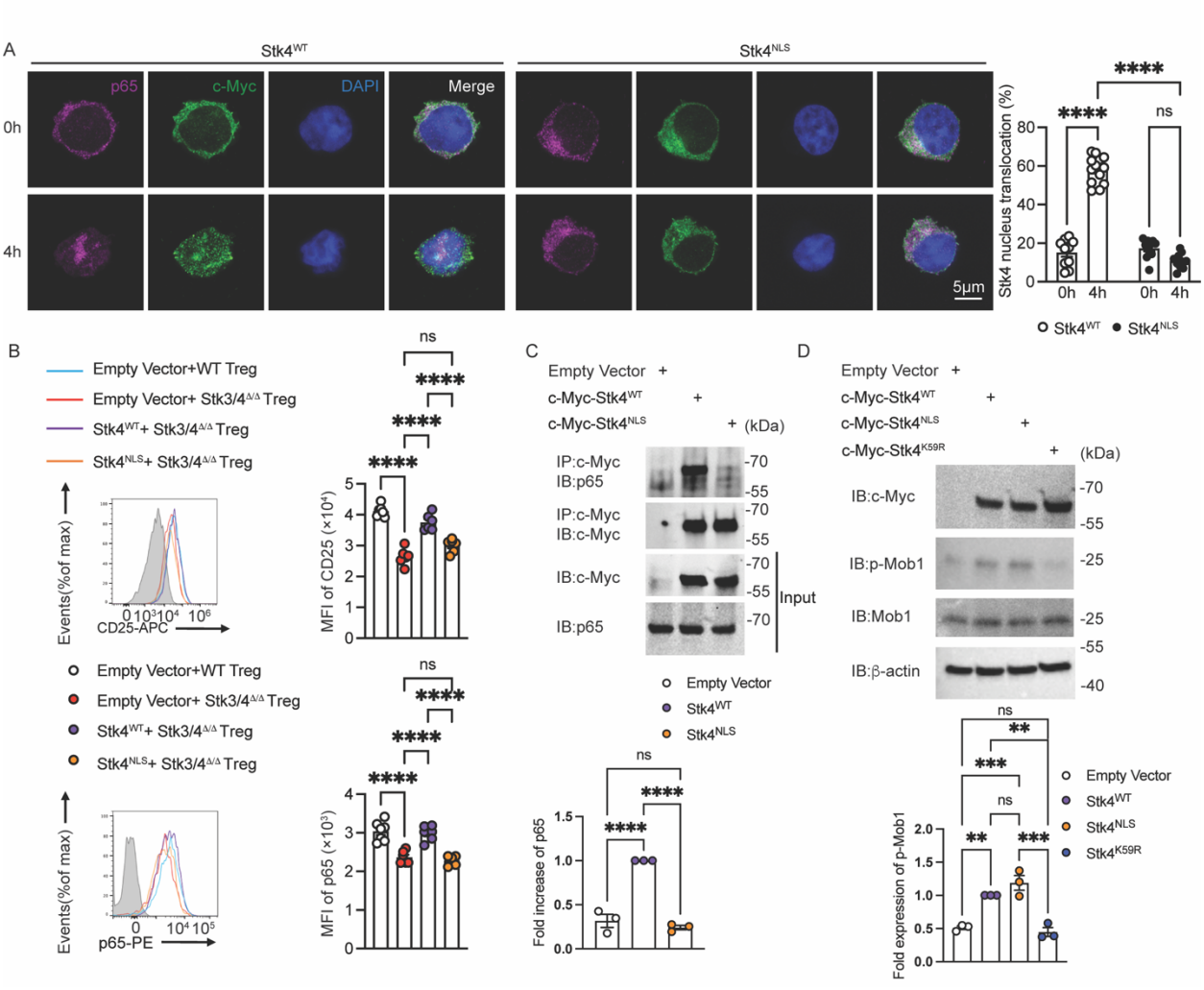

Fig. S6. The Stk4 NLS sequence is critical for Stk4-p65 interaction and CD25 upregulation in Treg cells. (A) Confocal microscopic analysis of p65, DAPI, and Stk4^{WT} or Stk4^{NLS} in unstimulated or stimulated cultures (4h) with anti-CD3/CD28 mAbs. **(B)** Flow cytometric analysis and scatter plot representation of CD25 (upper panel) or p65 (lower panel) analysis in *Foxp3*^{YFPCre} (WT) or *Foxp3*^{YFPCre}*Stk3/4*$^{Δ/Δ}$ Treg cells transfected with plasmids encoding Stk4^{WT} or Stk4^{NLS}. **(C)** Immunoblot analysis of Stk4 and p65 association in HEK293T cells transfected with the Stk4^{WT} or Stk4^{NLS}-encoding plasmids. Top: Cell lysates were immunoprecipitated with anti-c-Myc mAb, then immunoblotted with the indicated antibodies. Bottom: Densitometric analysis of immunoblots of p65 shown in

the top panel (**C**). **(D)** Top: Immunoblot analysis of p-Mob1 in HEK293T cells transfected with the Stk4^{WT} Stk4^{K59R}, or Stk4^{NLS}-encoding plasmids. Cell lysates were immunoblotted with the indicated antibodies. Bottom: densitometric analysis of immunoblots of p-Mob1 shown in the top panel. Each point represents one cell (A), one independent cell culture each from one mouse (B) or one immunoprecipitation (C and D). Error bars indicate the standard error of the means (S.E.M.). Statistical tests: Two-way ANOVA with post-test analysis (**A**), One way ANOVA with post-test analysis (B to D). ns: Not significant, **, *P*<0.01, ***, *P*<0.001, ****, *P*<0.0001.

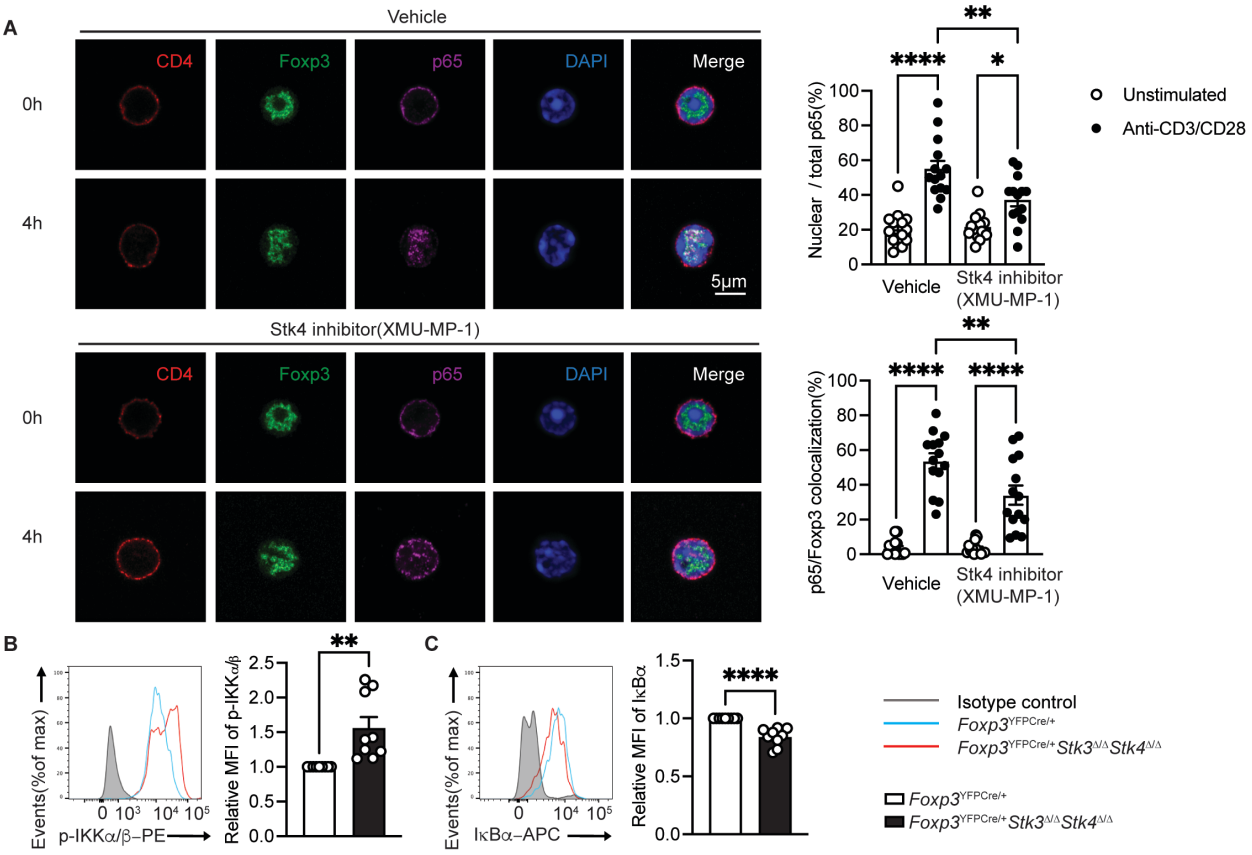

Fig. S7. Inhibition of Stk4 kinase activity attenuates the nuclear translocation of p65. (**A**) Confocal microscopic analysis of CD4, Foxp3, p65, DAPI and Merge and ratios of nuclear/total Stk4 in *Foxp3*^{YFPCre} Treg cell cultures either unstimulated or stimulated

with anti-CD3/CD28 mAbs without or with the Stk4 kinase inhibitor XMU-MP-1 (*n*=14 per group). (**B** to **C**) Representative flow cytometric analysis and scatter plot representation of p-IKKα/β (*n*=9 per group), IκBα MFI (*n*=9 per group) in *Foxp3*$^{YFPCre/+}$ and *Foxp3*$^{YFPCre/+}$*Stk3*$^{\Delta/\Delta}$*Stk4*$^{\Delta/\Delta}$ YFP^{+} Treg cells. Results represent pool of 3 independent experiments. Each point represents one mouse. Error bars indicate the standard error of the means (S.E.M.). Statistical tests: Student's unpaired two tailed *t* test (**B** and **C**) and two-way ANOVA with post-test analysis (**A**). ns: Not significant, *, $P<0.05$, **, $P<0.01$, ****, $P<0.0001$.

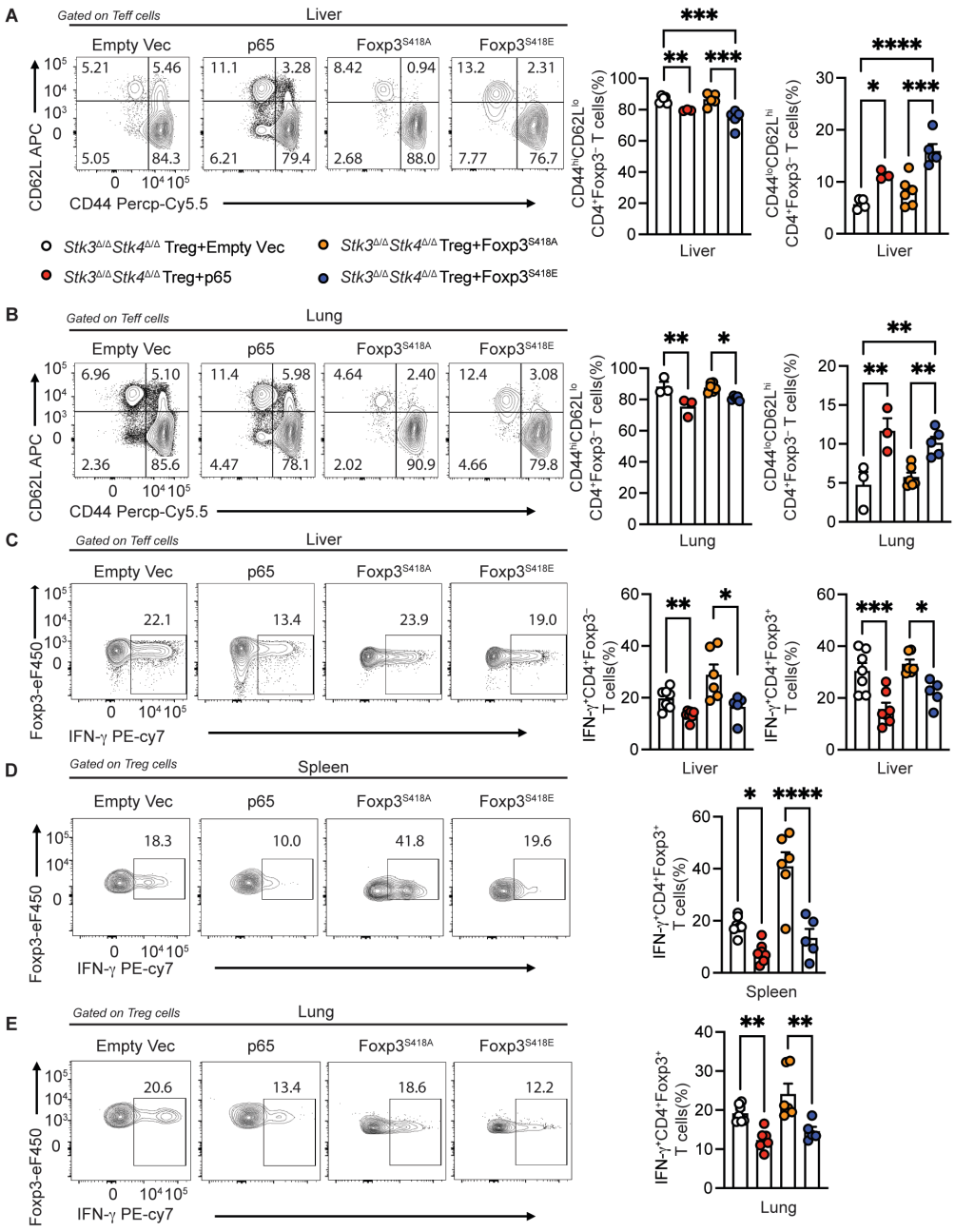

Fig. S8. p65 and Foxp3^{S418E} -transduced Treg cells ameliorate the disease of *Foxp3*$^{\Delta EGFPiCre}$ mice. (**A** and **B**) Representative flow cytometric analysis and cell frequencies of CD62L^{lo}CD44^{hi} CD4^{+}Foxp3^{-} Teff cells and CD62L^{hi}CD44^{lo} CD4^{+}Foxp3^{-} Teff cells from livers (*n*=5 for empty vector group; *n*=3 for p65 group; *n*=6 for Foxp3^{S418A} group; *n*=5 for Foxp3^{S418E} group) (A) and lungs (*n*=3 for empty vector group; *n*=3 for p65

group; *n*=6 for Foxp3^{S418A} group; *n*=5 for Foxp3^{S418E} group) (B) of *Foxp3*$^{\Delta EGFPiCre}$ mice injected with the respectively transduced *Foxp3*^{YFPCre}*Stk3*$^{\Delta/\Delta}$*Stk4*$^{\Delta/\Delta}$ Treg cells. The results were pooled from three independent experiments. (**C** to **E**) Representative flow cytometric analysis and cell frequencies of liver IFNγ$^+$ CD4$^+$Foxp3$^-$ Teff cells and IFNγ$^+$ CD4$^+$Foxp3$^+$ Treg cells (**C**), splenic IFNγ$^+$ CD4$^+$Foxp3$^+$ Treg cells (**D**) and lung IFNγ$^+$ CD4$^+$Foxp3$^+$ Treg cells from lungs (**E**) of each group (*n*=7 for empty vector group; *n*=7 for p65 group; *n*=6 for Foxp3^{S418A} group; *n*=5 for Foxp3^{S418E} group). The results were pooled from three independent experiments. Each point represents one mouse. Error bars indicate the standard error of the means (S.E.M.). Statistical tests: Student's unpaired two tailed *t* test (**A** to **C**) and one-way ANOVA with post-test analysis (**C** to **E**). ns: Not significant, *, *P*<0.05, **P<0.01.

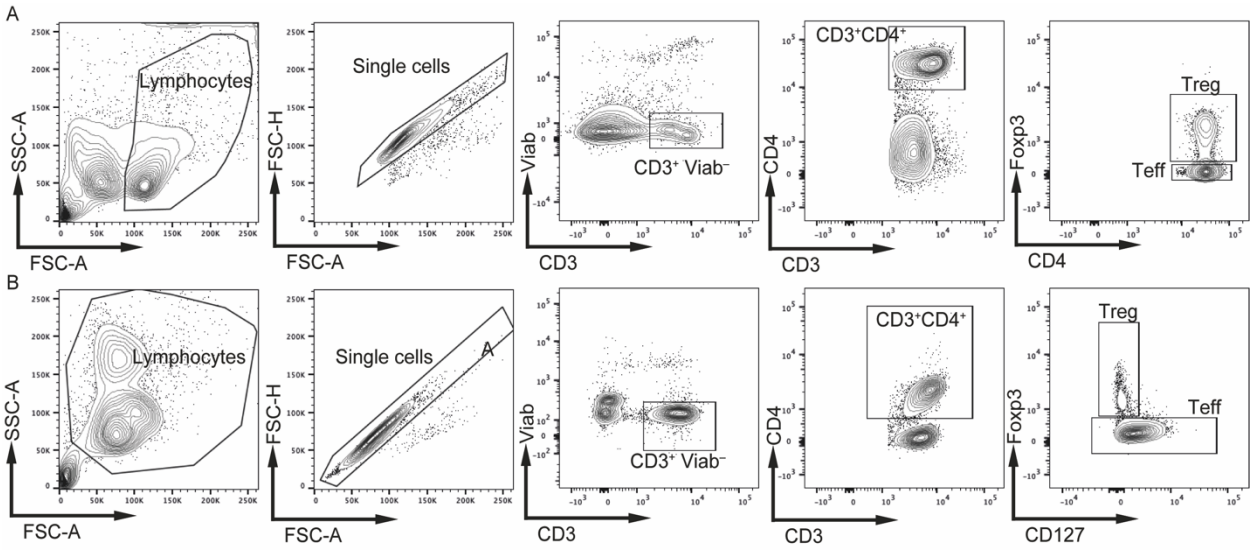

Fig. S9. Gating strategies for human and mouse Treg and Teff cell discrimination. (A) Mouse lymphocyte gating. Forward and side scatter (FSC and SSC) analysis of mouse splenocytes was followed by CD3 versus viability Dye (Viab) gating on single cells, then CD3 versus CD4 gating on CD3$^+$ Viability Dye$^-$ cells, and finally Foxp3 versus CD4

staining gated on $CD3^+CD4^+$ cells. (B) Human lymphocyte gating. Forward and side scatter (FSC and SSC) analysis of human mononuclear cells (PBMCs) was followed by CD3 versus viability Dye gated on single cells, then CD3 versus CD4 gated on $CD3^+$ Viability Dye^- cells, then Foxp3 versus CD127 staining, gated on $CD3^+CD4^+$ cells.

Table S1. Listing of flow cytometry antibodies used.

Marker	Fluorochro	clone	compagny	dilution	Staining
Foxp3	eF450	FJK-16S	eBioscience	1/500	Intracellular
	AF488	FJK-16S	eBioscience	1/500	Intracellular
CTLA4	PE	UC10-4B9	eBioscience	1/300	Intracellular
Helios	APC	22F6	eBioscience	1/300	Intracellular
IFN-γ	APC	XMG1.2	Biolegend	1/500	Intracellular
IL-17A	PE-Cy7	TC11-18H10.1	Biolegend	1/500	Intracellular
	APC	TC11-18H10.1	Biolegend	1/500	Intracellular
IL-4	PE	11B11	Biolegend	1/300	Intracellular
IL-10	AF700	JES5-16E3	eBioscience	1/300	Intracellular
CD4	BV605	GK1.5	Biolegend	1/500	Surface
	PE	GK1.5	Biolegend	1/500	Surface
CD8	PE	53-6.7	eBioscience	1/500	Surface
CD62L	APC	MEL-14	Biolegend	1/300	Surface
CD44	eF450	IM7	eBioscience	1/300	Surface
CD90.2	APC-Cy7	30-H12	Biolegend	1/500	Surface
CD90.1	APC-Cy7	OX-40	Biolegend	1/500	Surface
CD25	eF450	PC61	Biolegend	1/500	Surface
ICOS	PE	7E.17G9	eBiosceince	1/300	Surface
Nrp1	PE	3DS304M	eBioscience	1/300	Surface
CD73	APC	TY/11.8	Biolegend	1/300	Surface
Phospho-p65(Ser536)	PE	93H1	Cell Signaling	1/300	Intracellular
NF-κB p65	Alexa 647	D14E12	Cell Signaling	1/500	Intracellular
Phospho-IKKα/β (Ser176/180)	PE	16A6	Cell Signaling	1/500	Intracellular
IκBα	Alexa 647	L35A5	Cell Signaling	1/500	Intracellular
Viability dye	eFluor506		Biolegend	1/1000	Surface

Table S2. Listing of immunoblotting antibodies used.

Marker	Source	clone	compagny	dilution
Foxp3	Mouse	Polyclonal	MBL	1/500
Foxp3	Mouse	150D/E4	ebioscience	1/1000
NF-κB p65	Rabbit	D14E12	Cell signaling	1/1000
Phospho- NF-κB p65(Ser536)	Rabbit	93H1	Cell signaling	1/1000
Anti-Phosphoserine/threonine	Mouse	22A/pSer/Thr	BD	1/500
Phospho-FOXP3(S418)	Rabbit	Polyclonal	abgent	1/1000
MST1	Rabbit	D8B9Q	Cell signaling	1/1000

β-actin	Rabbit	13E5	Cell signaling	1/5000
V5	Mouse	Polyclonal	biolegend	1/1000
DYKDDDDK	Rabbit	D6W5B	Cell signaling	1/1000
c-Myc	Mouse	C-33	Santa Cruz	1/1000
Rabbit IgG-HRP	Goat	RPA-T4	Cell signaling	1/5000
Mouse IgG-HRP	Horse	NA	Cell signaling	1/5000

Table S3. Listing of software, package and tools used.

Software/Package/Tools	Version	Source
Bedtools	v2.27.1	https://github.com/arq5x/bedtools2/releases/tag/v2.27.1
Bowtie2	v2.3.4.3	https://github.com/BenLangmead/bowtie2/releases/download/v2.3.4.3/bowtie2-2.3.4.3-linux-x86_64.zip
ChIPseeker	v1.22.1	https://bioconductor.org/packages/ChIPseeker/
Cutadapt	v1.9.1	https://pypi.org/project/cutadapt/1.9.1/
ngs.plot	v2.63	https://github.com/shenlab-sinai/ngsplot
ENCODE blacklist regions		https://github.com/Boyle-Lab/Blacklist/
FastQC	v0.11.9	http://www.bioinformatics.babraham.ac.uk/projects/fastqc/fastq%0Ac_v0.11.5.zip
MACS2	v2.2.7.1	https://pypi.org/project/MACS2/
MultiQC	v1.9	https://pypi.org/project/multiqc/1.9/
Picard tools	v2.25.4	https://broadinstitute.github.io/picard/
Python	v.2.7/3.7	https://www.python.org/ftp/python/3.7.6/Python-3.7.6.tgz
R	v3.6.3	http://cran.r-project.org/src/base/R-3/R-3.6.3.tar.gz
Rstudio	v1.2.133	https://download1.rstudio.org/desktop/xenial/amd64/rstudio-%0A5 1.2.1335-amd64.deb
Samtools	v1.9	https://sourceforge.net/projects/samtools/files/samtools/1.9/sa%0Amtools-1.9.tar.bz2/download
TxDb.Mmusculus.UCSC.mm10.ensGene	v3.4.0	https://bioconductor.org/packages/TxDb.Mmusculus.UCSC.mm10.ensGene/
UCSC genome browser		https://genome.ucsc.edu/index.html